Magnetohydrodynamic Fluid Flow Past Contracting Surface in a Rotating System

Samuel K. Muondwe[a*], Mathew kinyanjui[b], David Theuri[c], Kang'ethe Giterere[d]

[a]*Dedan Kimathi University of Technology, Department of Mathematics and Physical Science, P.O Box 657, Nyeri*

[b,c,d]*Jomo Kenyatta University of Agriculture and Technology, Department of Pure and Applied Mathematics.P.0 BOX 62000, NAIROBI ,KENYA*

Abstract

Heat and mass transfer past a contracting surface in a rotating system has been discussed. In this study, the governing equations are transformed into a system of partial differential equations and solved numerically using finite difference method. The solutions are presented graphically for various parameters. The results obtained are applicable in areas such as polymer technology, metallurgy, cooling of metallic plates; control of boundary layer along a liquid film in condensation processes, cooling of micro electromechanical systems, shrink packaging, cooling of nuclear reactor.

Keywords: Rotation; radiation; contracting surfaces; MHD.

1. Introduction

Fluid is defined as a substance that deforms continuously when acted on by a shearing stress of any magnitude. Fluids can be characterized as Newtonian and non-Newtonian fluids. For Newtonian fluids the shearing stress is linearly related to the rate of shearing strain but for non-Newtonian fluids shearing stress is not linearly related to the rate of shearing strain. Water, air, mercury, kerosene and thin lubricating oils are Newtonian fluids whereas paints, coal tar, blood and grease represent for non-Newtonian fluids.

----

* Corresponding author.

Magnetohydrodynamics (MHD) is the science of the motion of electrically conducting fluids in presence of magnetic fields.MHD studies the dynamics of the interaction of electrically conducting fluids and the electromagnetic field. The fluids can be ionized gases (commonly known as plasma) or liquid metals. The flow of an electrically conducting fluid under a magnetic field in general gives rise to induced electric currents. The induced currents flow in the direction perpendicular to both the magnetic field and the direction of the motion of the fluid. The importance of studying fluid dynamics is the analysis of systems involving fluid flow, heat transfer and associated phenomena such as diffusion, convection, dissipation, boundary layers and turbulence by means of computer based simulation. All of these phenomena are governed by the compressible Navier-Stokes equations.

Some of applications of the boundary layer flow include wire drawing, paper production, glass-fiber production, liquid metal, polymer sheet synthesis, continuous stretching of plastic films and artificial fibers etc. In all these cases, the mechanical properties of the final product are appreciably affected by the rate of cooling and stretching in the process and material characteristics could therefore be manipulated to desired specifications [1].Flow due to a shrinking sheet is different from the stretching sheet flow. A stretching sheet regime induces far field suction towards the sheet, while a shrinking sheet intensifies the velocity away from the sheet. Shrinking sheet flows are important in the manufacture of certain polymers and high-performance materials for aerospace coatings [2].

Most researchers have studied wide variety of flow situations. Some of these studies can be found in work of [3] studied flow and heat transfer of a fluid through a porous medium over a stretching surface with internal heat generation/ absorption and suction/ blowing. [4] Studied thermal diffusion and chemical reaction effects on unsteady MHD free convection flow past a semi infinite vertical permeable moving plate. [5] investigated numerical steady free convection flow through a porous medium around a rectangular isothermal body. [6] studied free convective mass transfer flow past infinite vertical porous plate with Soret effect.

Following are some research on effects of radiation, heat generation and viscous dissipation [7] presented work on MHD free convection heat and mass transfers of a heat generations fluid past an impulsively started infinite porous plate with Hall currents and radiation absorption. [8] Studied combined effects of thermal radiation and hall current on MHD free-convective flow and mass transfer over a stretching sheet with Variable Viscosity. The study of MHD rotating system had considerable progress in the last few decades. For instance [9] studied MHD Flow in Porous Media over A Stretching Surface in Rotating System with Hall Currents, Heat and Mass Transfer.

Also researchers have analyzed problems of flow over shrinking surface under various conditions. [10] Studied effects of thermal radiation on MHD viscous fluid flow and heat transfer over non linear shrinking porous sheet. Reference [11] Studied combined effects of variable magnetic field and porous medium on the flow of MHD fluid due to exponentially shrinking sheet.

Less emphasis has been given to the problems of flow due to a contracting sheet. The aim of this work is therefore to investigate MHD stokes fluid flow problem and combined effects of various parameters on velocity,

temperature and concentration past a porous contracting surface in a rotating system.

2. Mathematical formulation

Consider flow of an incompressible, electrically conducting, and viscous Newtonian fluid past a contracting electrically non-conducting sheet embedded in porous media in a rotating system.

A second impermeable and electrically non conducting sheet is placed parallel to the contracting sheet for closed flow. The system is rotated with constant angular velocity Ω, the y axis is taken to be infinite. The surface of the contracting sheet is maintained at a uniform temperature T_w. The free stream temperature and concentration of spicies are T_∞ and C_∞ respectively. An upward flow is established along the surface when $T_w > T_\infty$ due to free convection; and there is a down flow when $T_\infty > T_w$
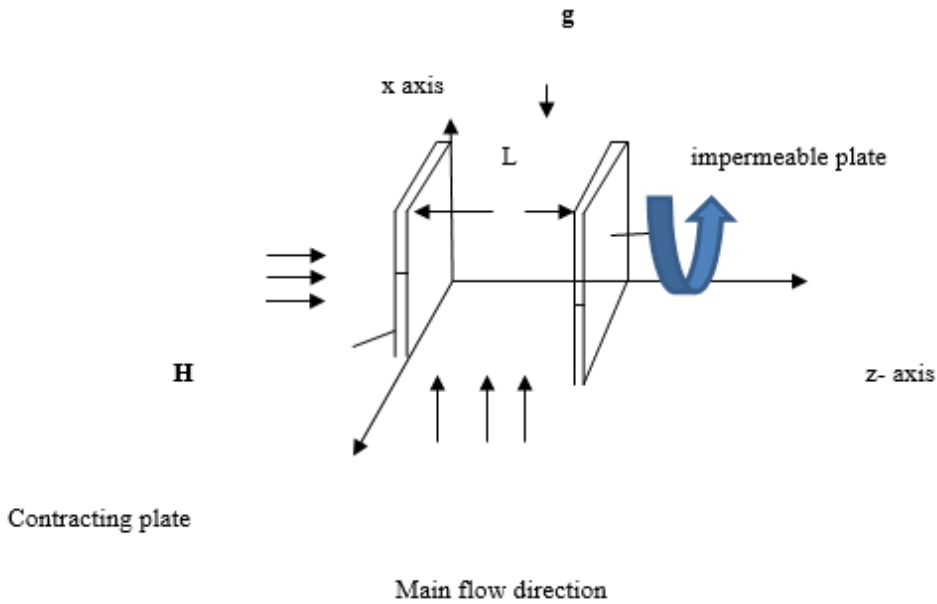
Figure 1.0: Flow configuration

The governing equations governing the flow are as follow:

$$\frac{\partial u}{\partial t} + u\frac{\partial u}{\partial x} + \omega_0 \frac{\partial u}{\partial z} - 2\Omega v = v\left(\frac{\partial^2 u}{\partial x^2} + \frac{\partial^2 u}{\partial z^2}\right) - u\frac{v}{k_p} + \frac{\sigma\mu^2 B^2 u}{\rho} + \beta g\left(T - T_\infty\right) + \beta^* g\left(C - C\infty\right)$$

(1)

$$\frac{\partial v}{\partial t} + u\frac{\partial v}{\partial x} + \omega_0 \frac{\partial v}{\partial z} + 2\Omega v = v\left(\frac{\partial^2 v}{\partial x^2} + \frac{\partial^2 v}{\partial z^2}\right) - v\frac{v}{k_p} - \frac{\sigma\mu^2 B^2 v}{\rho}$$

(2)

$$\frac{\partial T}{\partial t} + u\frac{\partial T}{\partial x} + \omega_0\frac{\partial T}{\partial z} = \frac{k_f}{\rho c_p}\left(\frac{\partial^2 T}{\partial x^2} + \frac{\partial^2 T}{\partial z^2}\right) + \frac{D_m k_T}{c_s c_p}\left(\frac{\partial^2 C}{\partial x^2} + \frac{\partial^2 C}{\partial z^2}\right)\frac{\mu}{\rho c_p}\left[\left(\frac{\partial u}{\partial z}\right)^2 + \left(\frac{\partial v}{\partial z}\right)^2\right]$$

$$+ \frac{\sigma\mu^2 B^2(u^2 + v^2)}{\rho c_p} - \frac{16\sigma^* T_\infty^3}{3\rho c_p k^*}\frac{\partial^2 T}{\partial z^2}$$

(3)

$$\frac{\partial C}{\partial t} + u\frac{\partial C}{\partial x} - \omega_0\frac{\partial C}{\partial z} = D_m\left(\frac{\partial^2 C}{\partial x^2} + \frac{\partial^2 C}{\partial z^2}\right) + \frac{D_m k_T}{T}\left(\frac{\partial^2 T}{\partial x^2} + \frac{\partial^2 T}{\partial z^2}\right) - u\frac{\partial C}{\partial x} + \omega_0\frac{\partial C}{\partial z}$$

(4)

The initial and boundary conditions of this problem are:

$$t \leq 0 : u = 0, v = 0, \omega = 0, T = 0, H = 0, C = 0 \text{ at } 0 \leq z \leq L$$

$$t > 0 : u = u_\infty, v = 0, T = T_\infty, C = C_\infty, H = H_0, at, x = 0 \text{ Channel entrance}$$

$$t > 0 : u = -cx^n, v = 0, T = T_w, C = C_w, H = H_0 x^{\frac{n-1}{2}}, at, z = 0 \text{ (porous wall)}$$

(5)

$$t > 0 : u = 0, v = 0, T = T_w, C = C_w, H = H_0, at, z = L \text{ (impermeable wall)}$$

Non-Dimensionalisation

Non-dimensionalizationis aimed at ensuring that the results are applicable to other geometrically similarly configurations under a similar set of flow conditions. The characteristic length is taken as perpendicular distance L units between the parallel sheets. The characteristic velocity is taken as the free stream velocity U_∞

The non-dimensional Variables are defined as follow;

$$u' = \frac{u}{U_\infty}, \ v' = \frac{v}{U_\infty}, \ \omega' = \frac{\omega_0}{U_\infty}, \ t' = \frac{U\infty t}{L}, \ z' = \frac{z}{L}, \ T' = \frac{T - T\infty}{T_w - T_\infty}$$

(6)

Governing equations in non dimensional form:

$$\frac{\partial u'}{\partial t'} + u'\frac{\partial u'}{\partial x'} - \omega'\frac{\partial u'}{\partial z'} - Rov' = \frac{1}{\text{Re}}\left(\frac{\partial^2 u'}{\partial x'^2} + \frac{\partial^2 u'}{\partial z'^2}\right) - Xiu' - Mu' + Gr_\theta T' + Gr_c C'$$

(7)

$$\frac{\partial v'}{\partial t'} + u'\frac{\partial v'}{\partial x'} - \omega'\frac{\partial v'}{\partial z'} + Rou' = \frac{1}{\text{Re}}\left(\frac{\partial^2 v'}{\partial x'^2} + \frac{\partial^2 v'}{\partial z'^2}\right) - Xiv' - Mv''$$

(8)

$$\frac{\partial T^{'}}{\partial t^{'}} + u^{'}\frac{\partial T^{'}}{\partial x^{'}} - \omega_0 \frac{\partial T^{'}}{\partial z^{'}} = \frac{1}{\text{Re}}\left[\frac{1}{pr}\left(\frac{\partial^2 T^{'}}{\partial x^{'2}} + \frac{\partial^2 T^{'}}{\partial z^{'2}}\right)\right] + D_f \text{Re}\left(\frac{\partial^2 C^{'}}{\partial x^{'2}} + \frac{\partial^2 C^{'}}{\partial z^{'2}}\right) + \frac{Ec}{\text{Re}}\left[\left(\frac{\partial u^{'}}{\partial z^{'}}\right)^2 + \left(\frac{\partial v^{'}}{\partial z^{'}}\right)^2\right]$$

$$-\frac{4}{3N\,\text{Pr}\,\text{Re}}\left(\frac{\partial^2 T^{'}}{\partial z^{'2}}\right) + R\,\text{Re}\left(u^{'2} + v^{'2}\right)$$

$$(9)$$

$$\frac{\partial C^{'}}{\partial t^{'}} + u^{'}\frac{\partial C^{'}}{\partial x^{'}} - \omega\frac{\partial C^{'}}{\partial z^{'}} = \frac{1}{\text{Re}\,Sc}\left(\frac{\partial^2 C^{'}}{\partial x^{'2}} + \frac{\partial^2 C^{'}}{\partial z^{'2}}\right) + \frac{Sr}{\text{Re}}\left(\frac{\partial^2 T^{'}}{\partial x^{'2}} + \frac{\partial^2 T^{'}}{\partial z^{'2}}\right) \qquad (10)$$

Where $M = \dfrac{\sigma \mu_e^2 H^2}{\rho U_\infty}$ is the magnetic field parameter, $\text{Re} = \dfrac{U_\infty L}{\vartheta}$ is the Reynolds number, $Xi = \dfrac{\vartheta L}{U_\infty k_p}$ is

the permeability parameter, $Gr_\theta = \dfrac{\beta g L (T_w - T_\infty)}{U_\infty^2}$ is the local temperature Grashof number, $Ro = \dfrac{2\Omega}{U_\infty^2}$ is

rotational parameter, Where $\text{Pr} = \dfrac{\mu c_p}{k_f}$ is prandlt number, $N = \dfrac{k^* k_f}{4\sigma^* T_\infty^3}$ is the radiation parameter,

$D_f = \dfrac{\rho D_m k_f (C_w - C_\infty)}{\mu c_s c_p (T_w - T_\infty)}$ is Dufour number , $Ec = \dfrac{U^2}{c_p \Delta T}$ is the Eckert number, $R = \dfrac{\sigma \mu_e^2 H^2}{\rho^2 c_p \Delta T}$ is the

Joule heating parameter and ΔT represents the temperature differences. $(T_w - T_\infty)$.

Where $Sc = \dfrac{\mu}{\rho D_m}$ is the schimidt number, $Sr = \dfrac{\rho D_m k_f (T_w - T_\infty)}{\mu T_m (C_w - C_\infty)}$ is the soret number

The initial and boundary conditions in non-dimensional form:

$$t^{'} < 0: u^{'} = 0, v^{'} = 0, T^{'} = 0, C^{'} = 0, H^{'} = 0, at, z = 0 \text{ at } 0 \leq z \leq L$$

$$t^{'} > 0: u^{'} = 1, v^{'} = 0, T^{'} = 1, C^{'} = 1, H^{'} = 1, at, z = 0 \text{ Channel entrance}$$

$$t^{'} > 0: u^{'} = \frac{-cLx^n}{U_\infty}, v^{'} = 0, T^{'} = 1, C^{'} = 1, H^{'} = x^{\frac{n-1}{2}}, at, z = 0 \text{ (porous wall)} \qquad (11)$$

$$t^{'} > 0: u^{'} = 0, v^{'} = 0, T^{'} =, C^{'} = 1, H^{'} = 1, at, z = L \text{ (Impermeable wall)}$$

3. Methodology

Equations that govern MHD flow past contracting surface in a rotating system with heat and mass transfer

transfers are non-linear. The equations are solved using finite differences method that applies Crank-Nicholson algorithm. The finite difference method replaces each PDE with a discrete approximation for space and time domain. Governing equations in finite difference form.

$$\frac{U_{i,j}^{k+1}-U_{i,j}^{k}}{\Delta t}+U_{i,j}^{k}\left(\frac{U_{i,j}^{k+1}-U_{i-1,j}^{k}+U_{i,j}^{k}-U_{i-1,j}^{k}}{2\Delta x}\right)-w_0\left(\frac{U_{i,j}^{k+1}-U_{i-1,j}^{k}+U_{i,j}^{k}-U_{i-1,j}^{k}}{2\Delta z}\right)-\frac{R_0}{2}\left(V_{i,j}^{k+1}+V_{i,j}^{k}\right)$$

$$=\frac{1}{2(\Delta x)^2\,\mathrm{Re}}\left(U_{i+1,j}^{k+1}-2U_{i,j}^{k+1}+U_{i-1,j}^{k+1}+U_{i+1,j}^{k}-2U_{i,j}^{k}+U_{i-1,j}^{k}\right)+\frac{1}{2(\Delta z)^2\,\mathrm{Re}}\left(U_{i+1,j}^{k+1}-2U_{i,j}^{k+1}+U_{i-1,j}^{k+1}+U_{i+1,j}^{k}-2U_{i,j}^{k}+U_{i-1,j}^{k}\right)$$

$$-\frac{Xi}{2}\left(U_{i,j}^{k+1}+U_{i,j}^{k}\right)-\frac{M}{2}\left(U_{i,j}^{k+1}+U_{i,j}^{k}\right)+\frac{Gr_\theta}{2}\left(T_{i,j}^{k+1}+T_{i,j}^{k}\right)+\frac{Gr_c}{2}\left(C_{i,j}^{k+1}+C_{i,j}^{k}\right)$$

(12)

$$\frac{V_{i,j}^{k+1}-V_{i,j}^{k}}{\Delta t}+U_{i,j}^{k}\left(\frac{V_{i,j}^{k+1}-V_{i-1,j}^{k}+V_{i,j}^{k}-V_{i-1,j}^{k}}{2\Delta x}\right)-w_0\left(\frac{V_{i,j}^{k+1}-V_{i-1,j}^{k}+V_{i,j}^{k}-V_{i-1,j}^{k}}{2\Delta z}\right)$$

$$+\frac{R_0}{2}\left(U_{i,j}^{k+1}+U_{i,j}^{k}\right)=\frac{1}{2(\Delta x)^2\,\mathrm{Re}}\left(V_{i+1,j}^{k+1}-2V_{i,j}^{k+1}+V_{i-1,j}^{k+1}+V_{i+1,j}^{k}-2V_{i,j}^{k}+V_{i-1,j}^{k}\right)$$

$$+\frac{1}{2(\Delta z)^2\,\mathrm{Re}}\left(V_{i+1,j}^{k+1}-2V_{i,j}^{k+1}+V_{i-1,j}^{k+1}+V_{i+1,j}^{k}-2V_{i,j}^{k}+V_{i-1,j}^{k}\right)-\frac{Xi}{2}\left(V_{i,j}^{k+1}+V_{i,j}^{k}\right)-\frac{M}{2}\left(V_{i,j}^{k+1}+V_{i,j}^{k}\right)$$

(13)

$$V_{i,j}^{k+1}=V_{i,j}^{k}+\frac{\Delta t}{2(\Delta x)^2\,\mathrm{Re}}\left(V_{i+1,j}^{k+1}+V_{i-1,j}^{k+1}+V_{i+1,j}^{k}-2V_{i,j}^{k}+V_{i-1,j}^{k}\right)+\frac{\Delta t}{2(\Delta z)^2\,\mathrm{Re}}\left(V_{i+1,j}^{k+1}+V_{i-1,j}^{k+1}+V_{i+1,j}^{k}-2V_{i,j}^{k}+V_{i-1,j}^{k}\right)$$

$$+\frac{\Delta t}{2\Delta x}U_{i,j}^{k}\left(V_{i-1,j}^{k+1}-V_{i,j}^{k}+V_{i-1,j}^{k}\right)+\frac{\Delta t w_0}{2\Delta z}\left(V_{i-1,j}^{k+1}-V_{i,j}^{k}+V_{i-1,j}^{k}\right)-\frac{\Delta t Xi}{2}V_{i,j}^{k}-\frac{\Delta t M}{2}V_{i,j}^{k}$$

$$+\frac{\Delta t R_0}{2}\left(U_{i,j}^{k+1}+U_{i,j}^{k}\right)/(1+\frac{\Delta t}{2\Delta x}V_{i,j}^{k}-\frac{w_0\Delta t}{2\Delta z}+\frac{\Delta t}{\mathrm{Re}(\Delta z)^2}+\frac{\Delta t}{\mathrm{Re}(\Delta x)^2}+\frac{\Delta t Xi}{2}+\frac{\Delta t M}{2})$$

(14)

$$\frac{T_{i,j}^{k+1}-T_{i,j}^{k}}{\Delta t}+U_{i,j}^{k}\left(\frac{T_{i,j}^{k+1}-T_{i-1,j}^{k}+T_{i,j}^{k}-T_{i-1,j}^{k}}{2\Delta x}\right)-w_0\left(\frac{T_{i,j}^{k+1}-T_{i-1,j}^{k}+T_{i,j}^{k}-T_{i-1,j}^{k}}{2\Delta z}\right)$$

$$=\frac{1}{2(\Delta x)^2\,\mathrm{Pr}\,\mathrm{Re}}\left(T_{i+1,j}^{k+1}-2T_{i,j}^{k+1}+T_{i-1,j}^{k+1}+T_{i+1,j}^{k}-2T_{i,j}^{k}+T_{i-1,j}^{k}\right)$$

$$+\frac{1}{2(\Delta z)^2\,\mathrm{Pr}\,\mathrm{Re}}\left(T_{i+1,j}^{k+1}-2T_{i,j}^{k+1}+T_{i-1,j}^{k+1}+T_{i+1,j}^{k}-2T_{i,j}^{k}+T_{i-1,j}^{k}\right)+\frac{Ec}{\mathrm{Re}}\left[\left(\frac{U_{i,j}^{k+1}-U_{i-1,j}^{k+1}+U_{i,j}^{k}-U_{i-1,j}^{k}}{2\Delta x}\right)^2+\left(\frac{V_{i,j}^{k+1}-V_{i-1,j}^{k+1}+V_{i,j}^{k}-V_{i-1,j}^{k}}{2\Delta z}\right)^2\right]$$

$$-\frac{2}{3Ni\,\mathrm{Pr}\,\mathrm{Re}(\Delta z)^2}\left(T_{i+1,j}^{k+1}-2T_{i,j}^{k+1}+T_{i-1,j}^{k+1}+T_{i+1,j}^{k}-2T_{i,j}^{k}+T_{i-1,j}^{k}\right)+R\,\mathrm{Re}\left[\left(\frac{U_{i,j}^{k+1}+U_{i,j}^{k}}{2}\right)^2+\left(\frac{V_{i,j}^{k+1}+V_{i,j}^{k}}{2}\right)^2\right]$$

$$+D_f\,\mathrm{Re}\left(\frac{C_{i+1,j}^{k+1}-2C_{i,j}^{k+1}+C_{i-1,j}^{k+1}+C_{i+1,j}^{k}-2C_{i,j}^{k}+C_{i-1,j}^{k}}{2(\Delta x)^2}\right)+D_f\,\mathrm{Re}\left(\frac{C_{i+1,j}^{k+1}-2C_{i,j}^{k+1}+C_{i-1,j}^{k+1}+C_{i+1,j}^{k}-2C_{i,j}^{k}+C_{i-1,j}^{k}}{2(\Delta z)^2}\right)$$

(15)

$$\frac{C_{i,j}^{k+1} - C_{i,j}^{k}}{\Delta t} + U_{i,j}^{k}\left(\frac{C_{i,j}^{k+1} - C_{i-1,j}^{k+1} + C_{i,j}^{k} - C_{i-1,j}^{k}}{2\Delta x}\right) - w_0\left(\frac{C_{i,j}^{k+1} - C_{i-1,j}^{k+1} + C_{i,j}^{k} - C_{i-1,j}^{k}}{2\Delta z}\right)$$

$$= \frac{1}{2(\Delta x)^2 Sc\,\mathrm{Re}}\left(C_{i+1,j}^{k+1} - 2C_{i,j}^{k+1} + C_{i-1,j}^{k+1} + C_{i+1,j}^{k} - 2C_{i,j}^{k} + C_{i-1,j}^{k}\right)$$

$$+ \frac{1}{2(\Delta z)^2 Sc\,\mathrm{Re}}\left(C_{i+1,j}^{k+1} - 2C_{i,j}^{k+1} + C_{i-1,j}^{k+1} + C_{i+1,j}^{k} - 2C_{i,j}^{k} + C_{i-1,j}^{k}\right)$$

$$+ \frac{Sr}{\mathrm{Re}}\left[\left(\frac{T_{i+1,j}^{k+1} - 2T_{i,j}^{k+1} + T_{i-1,j}^{k+1} + T_{i+1,j}^{k} - 2T_{i,j}^{k} + T_{i-1,j}^{k}}{2(\Delta x)^2}\right) + \left(\frac{T_{i+1,j}^{k+1} - 2T_{i,j}^{k+1} + T_{i-1,j}^{k+1} + T_{i+1,j}^{k} - 2T_{i,j}^{k} + T_{i-1,j}^{k}}{2(\Delta z)^2}\right)\right]$$

(16)

4. Discussion of the results

Various parameters that have been varied include the Reynold's number Re, Rotational parameter Ro, Permeability parameter Xi, local mass Grashof number , time t, Dufour number Df, Nusselt number Nu, Eckert number Ec, Soret number Sr, Schmidt number Sc, and suction parameter .

Velocity vs Distance along the plate.

curve	M	Ro	t	wo
v	100	5	0.000225	0.5
vi	80	5	0.000225	0.5
vii	50	5	0.000225	0.5
iv	100	10	0.000225	0.5
iii	100	15	0.000225	0.5
viii	100	5	0.000325	0.5
ix	100	5	0.000425	0.5
ii	100	5	0.000225	1.5
i	100	5	0.000225	2.5
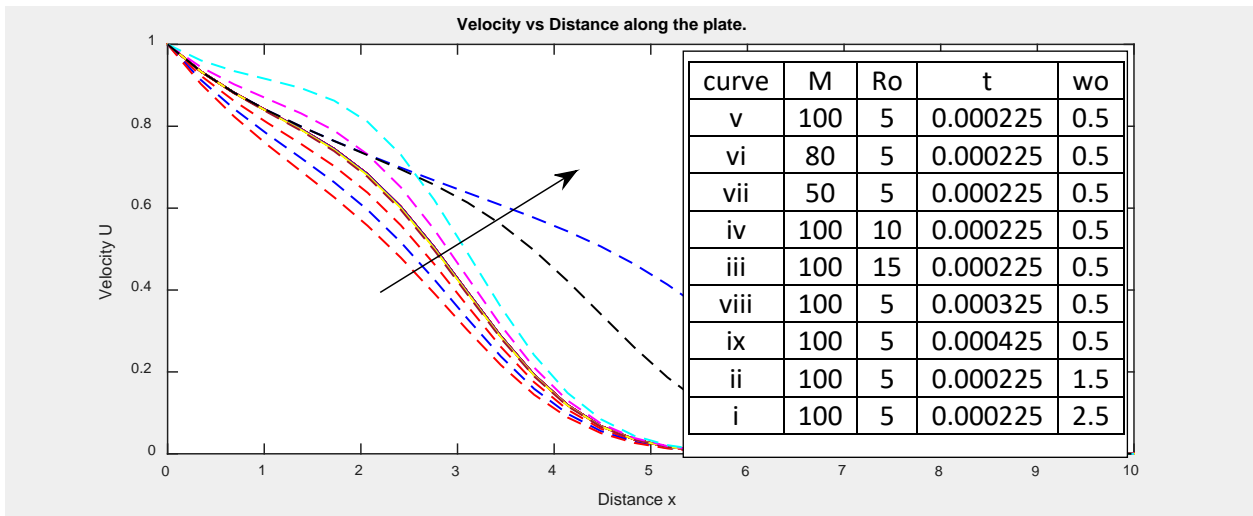
Figure 2.0: Primary velocity profiles for different values of Magnetic parameter M, rotation parameter, time and suction parameter W_0, for Grashof number $Gr_\theta = -0.5$

From figure 2 and 3 it is noted that increase in Magnetic parameter lead to a decrease in both primary and secondary velocity profiles. An increase in rotation parameter lead to a decrease in primary velocity profiles and an increase in secondary velocity profiles. Increase in time causes an increase in primary and secondary velocity. Increase in suction parameter causes a decrease in primary velocity profile and secondary velocity profiles.

Velocity vs Distance along the plate.

curve	M	Ro	t	wo
v	100	5	0.000225	0.5
vi	80	5	0.000225	0.5
vii	50	5	0.000225	0.5
ii	100	10	0.000225	0.5
i	100	15	0.000225	0.5
iv	100	5	0.000325	0.5
iii	100	5	0.000425	0.5
viii	100	5	0.000225	1.5
ix	100	5	0.000225	2.5
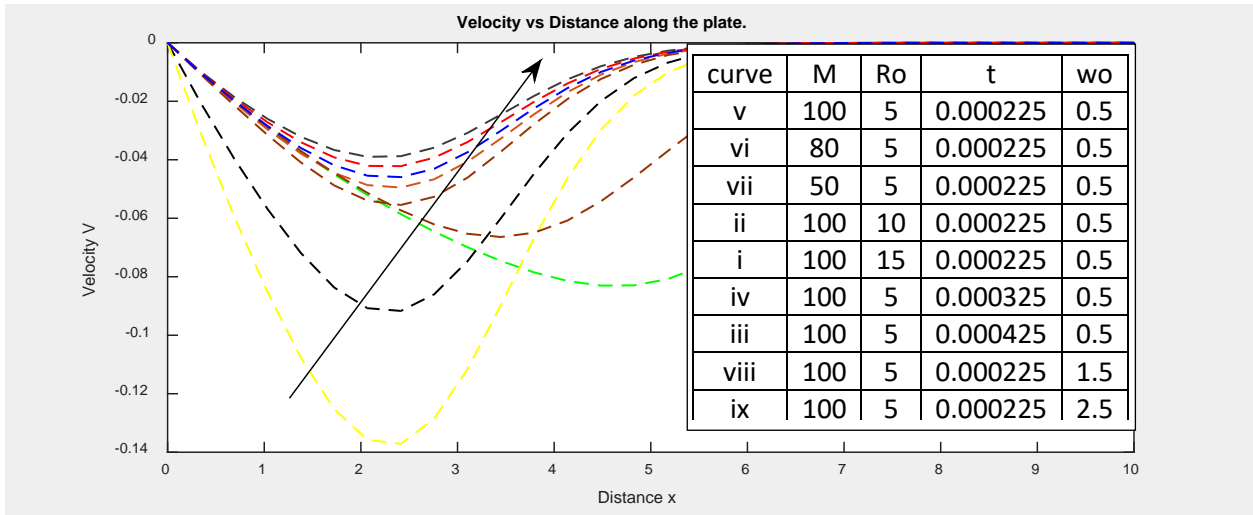
Figure 3: Secondary velocity profiles for different values of Magnetic parameter M, rotation parameter, time and suction parameter W_0, for Grashof number $Gr_\theta = -0.5$.

Temperature vs Distance along the plate.

curve	M	Ro	t	wo
vii	100	5	0.000225	0.5
Viii	80	5	0.000225	0.5
ix	50	5	0.000225	0.5
iv	100	10	0.000225	0.5
ii	100	15	0.000225	0.5
vi	100	5	0.000325	0.5
v	100	5	0.000425	0.5
iii	100	5	0.000225	1.5
i	100	5	0.000225	2.5
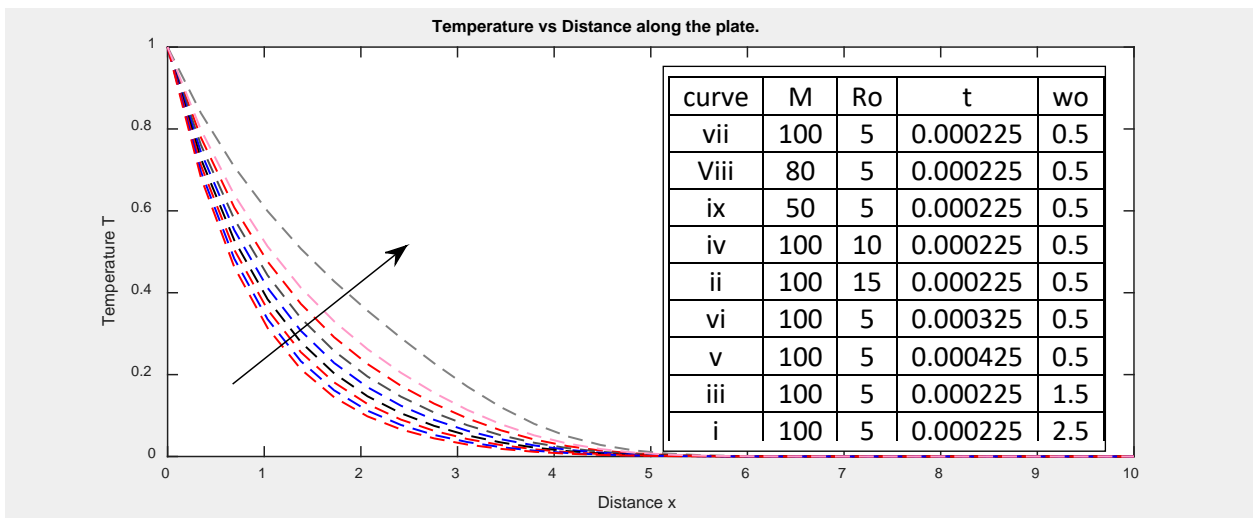
Figure 4: Temperature profiles for different values of Magnetic parameter M, rotation parameter, time and suction parameter W_0, for Grashof number $Gr_\theta = -0.5$.

From figure 4 it is noted that increase in M causes a decrease in the temperature profiles. The temperature profiles decrease with increasing M. The reduced velocity by the frictional drag due to the Lorentz force is responsible for reducing thermal viscous dissipation in the fluid leading to a thinner thermal boundary layer. An increase in Ro causes a decrease in the temperature profiles. An increase in time decreases the temperature. An increase in the magnitude of the suction parameter causes a decrease in the temperature profiles.

Concetration vs Distance along the plate.

curve	M	Ro	t	wo
vii	100	5	0.000225	0.5
vi	80	5	0.000225	0.5
v	50	5	0.000225	0.5
viii	100	10	0.000225	0.5
ix	100	15	0.000225	0.5
iv	100	5	0.000325	0.5
iii	100	5	0.000425	0.5
ii	100	5	0.000225	1.5
i	100	5	0.000225	2.5
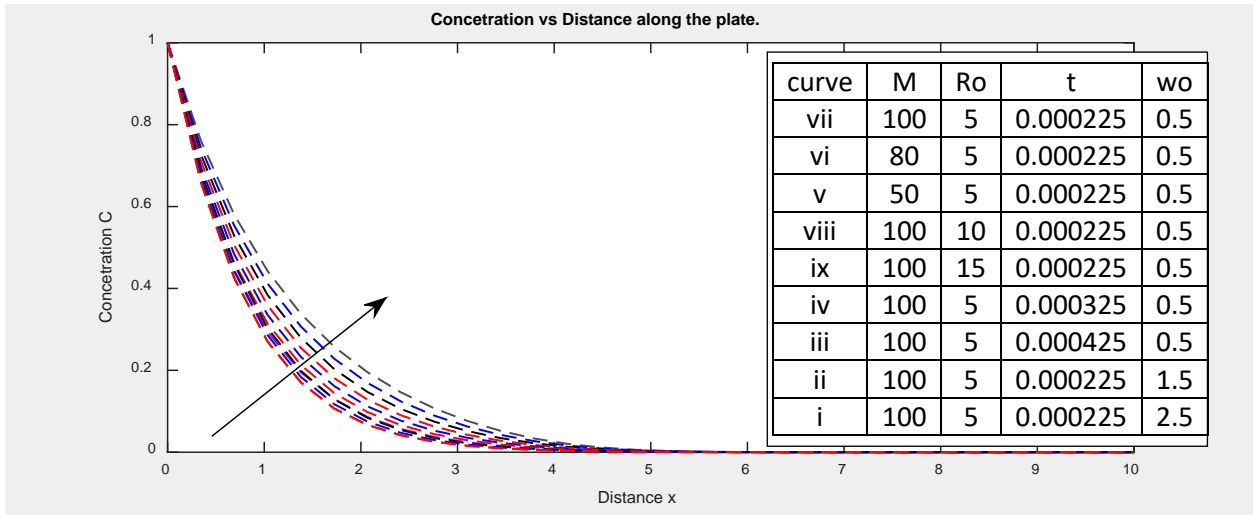
Figure 5: Concentration profiles for different values of Magnetic parameter M, rotation parameter, time and suction parameter W_0, for Grashof number $Gr_\theta = -0.5$.

From figure 5 it is noted that an increase in M causes an increase in the concentration profiles. An increase in Ro causes an increase in the concentration profiles. An increase in time decreases the concentration profiles. An increase in the magnitude of the suction parameter causes a decrease in the concentration profiles.

Velocity vs Distance along the plate.

curves	Xi	Ni	Re	Pr
v	0.5	0.5	3	0.7
iv	1.5	0.5	3	0.7
iii	3.5	0.5	3	0.7
vi	0.5	5	3	0.7
vii	0.5	15	3	0.7
ii	0.5	0.5	4	0.7
i	0.5	0.5	6	0.7
v	0.5	0.5	3	0.64
vii	0.5	0.5	3	7
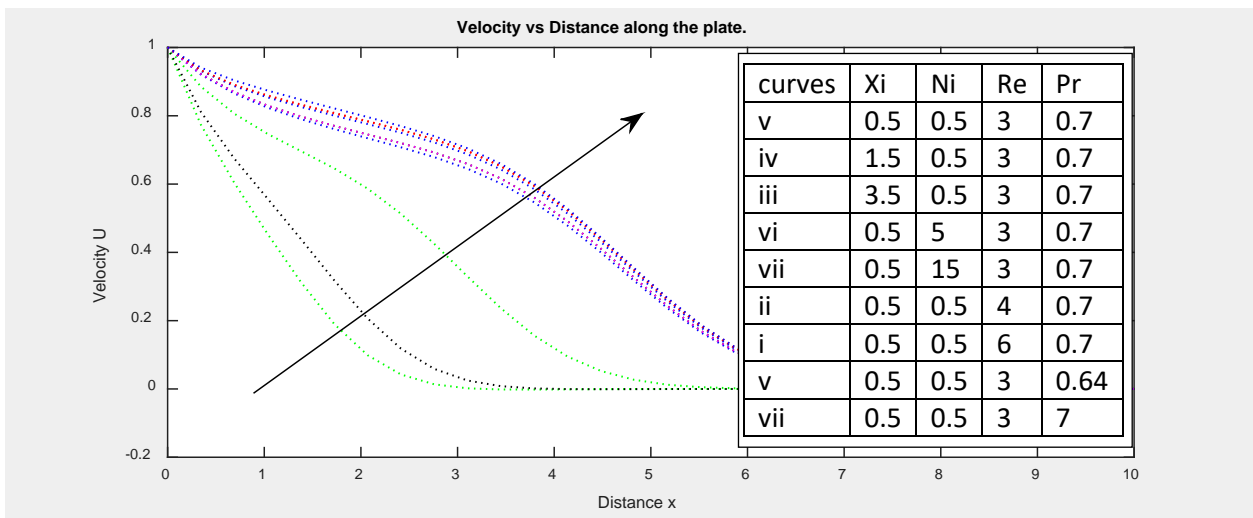
Figure 6: Primary velocity profiles for different values of permeability parameter X_i, radiation parameter N, Reynolds number Re, Prandtl number Pr for $Gr_\theta = -0.5$.

From Figure 6 and 7 it is noted that an increase in permeability Xi causes a decrease in the primary velocity and secondary velocity profiles respectively. The permeability parameter Xi is inversely proportional to the actual permeability k_p of the porous medium. Increase in Xi leads to deceleration of the flow hence the velocity decreases. Increasing Xi, increases the resistance of the porous medium (as the permeability physically becomes less with increasing Xi). This decelerates the flow and reduces the magnitudes of both the primary and

secondary velocity respectively. An increase in radiation parameter N leads to increase in primary velocity profiles and secondary velocity profiles respectively. Increase in Reynolds' number Re causes a decrease in the primary and secondary velocity profiles and then to an increase due to cross over. The Reynolds's number represents the ratio of the inertial to viscosity forces.

curves	Xi	Ni	Re	Pr
iv	0.5	0.5	3	0.7
v	1.5	0.5	3	0.7
vi	3.5	0.5	3	0.7
iii	0.5	5	3	0.7
i	0.5	15	3	0.7
viii	0.5	0.5	4	0.7
ix	0.5	0.5	6	0.7
vii	0.5	0.5	3	0.64
ii	0.5	0.5	3	7
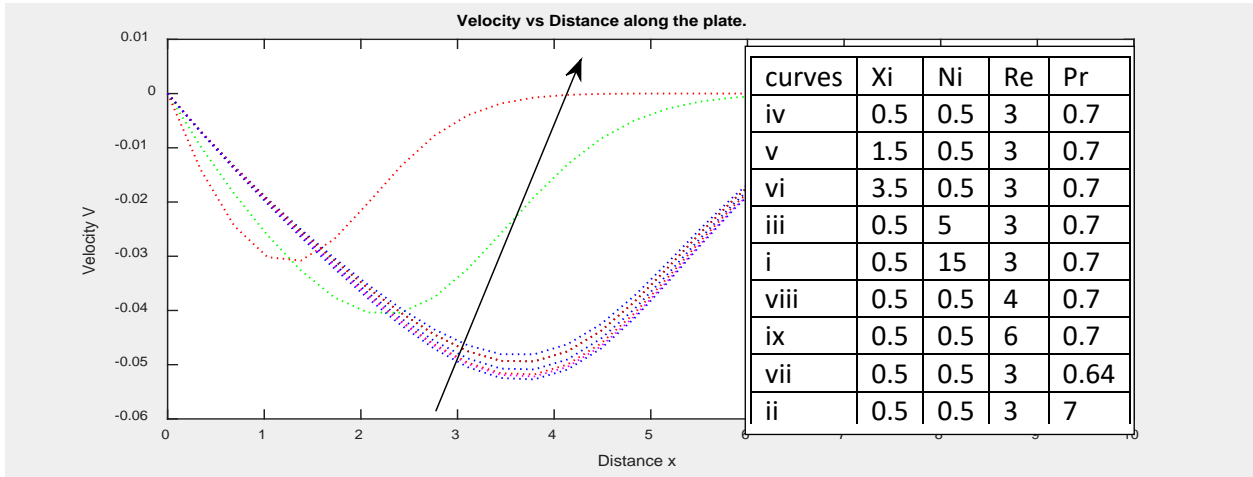
Figure 7: Secondary velocity profiles for different values of permeability parameter X_i, radiation parameter N,

Reynolds number Re, Prandtl number Pr for $Gr_\theta = -0.5$

curves	Xi	Ni	Re	Pr
v	0.5	0.5	3	0.7
iii	1.5	0.5	3	0.7
ii	3.5	0.5	3	0.7
ii	0.5	5	3	0.7
i	0.5	15	3	0.7
vi	0.5	0.5	4	0.7
vii	0.5	0.5	6	0.7
vi	0.5	0.5	3	0.64
iv	0.5	0.5	3	7
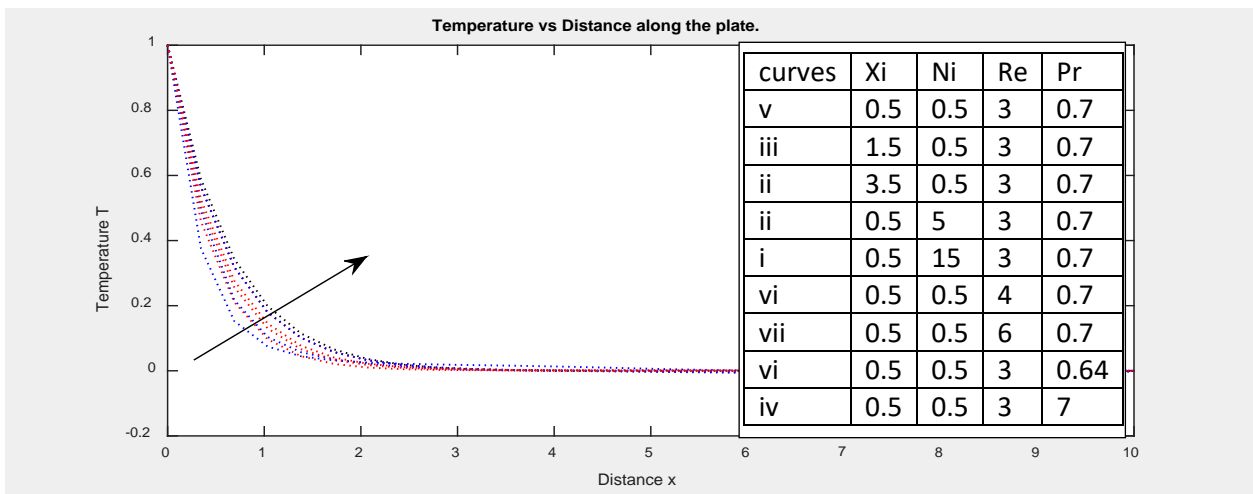
Figure 8: Temperature profiles for different values of permeability parameter X_i, radiation parameter N,

Reynolds number Re, Prandtl number Pr for $Gr_\theta = -0.5$

Increase in Re results to a large inertial force that in turn translates to a higher velocity. An increase in Prandtl number causes an increase of both primary and secondary velocity profiles. It's higher in water as compared to air and gases.

From figure 8 it is noted that an increase in permeability Xi causes a decrease in the temperature profiles. An increase in N leads to a decrease in the temperature profiles. An increase in Reynolds's number causes increase

in temperature profiles. An increase in Prandtl number causes a decrease in temperature profiles.

Concetration vs Distance along the plate.

curves	Xi	Ni	Re	Pr
v	0.5	0.5	3	0.7
vii	1.5	0.5	3	0.7
viii	3.5	0.5	3	0.7
vi	0.5	5	3	0.7
ix	0.5	15	3	0.7
iii	0.5	0.5	4	0.7
ii	0.5	0.5	6	0.7
i	0.5	0.5	3	0.64
iv	0.5	0.5	3	7
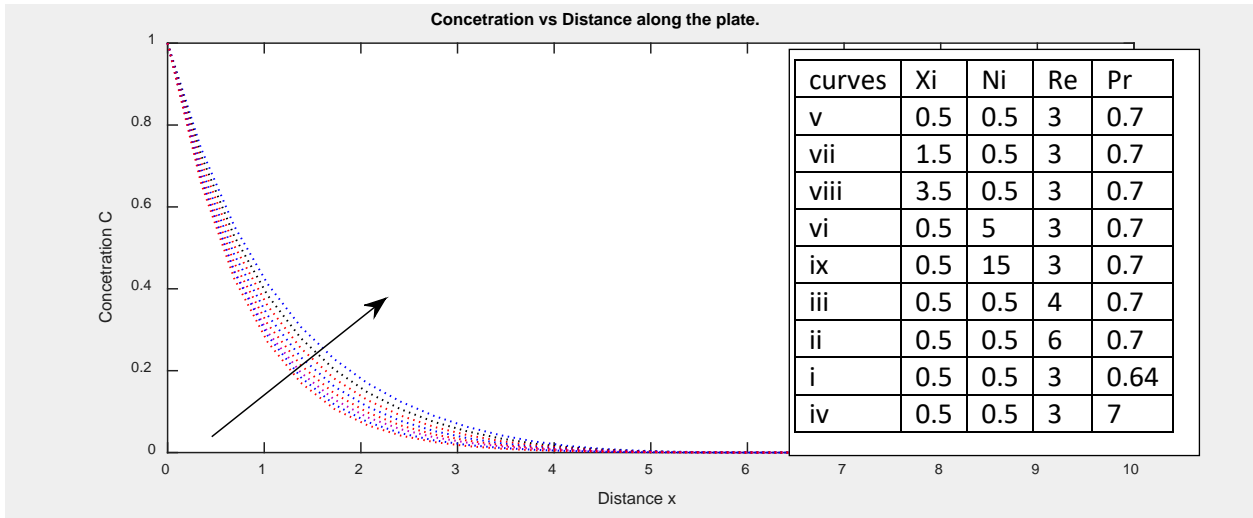
Figure 9: Concentration profiles for different values of permeability parameter X_i, radiation parameter N,

Reynolds number Re, Prandtl number Pr for $Gr_\theta = -0.5$

From figure 9 it is noted that an increase in Xi reduces the rate of species transportation from the surface of the contracting sheet, leading to an increase in the concentration profiles. An increase in N leads to an increase in the concentration profiles.

An increase in Re causes a decrease in the concentration profiles. A higher velocity of the fluid takes away more species from the surface of the contracting sheet thereby reducing the species concentration. Increase in Prandtl number causes a decrease in concentration profiles. From figure 10 and 11 it is noted that an increase in the Dufour number Df causes decrease in the primary and secondary velocity profiles. An increase in Schmidt number Sc causes a decrease in primary profiles and secondary velocity profiles. A large value of Sc means a presence of a heavier fluid and this implies a lower velocity of the fluid. An increase in Sr causes a decrease in the primary and secondary velocity profiles. An increase in Eckert number Ec causes an increase in the primary and secondary velocity profiles. The Eckert number expresses the relationship between the kinetic energy in the flow and the enthalpy. It embodies the conversion of kinetic energy into internal energy by work done against the viscous fluid stresses. A positive Eckert number implies cooling the sheet, implying heating the fluid. This causes a rise in the velocity of the fluid respectively.

From figure 12 it is noted that an increase in Df causes a decrease in the temperature profiles. The Dufour number signifies the contribution of the concentration gradients to the thermal energy flux in the flow. From the definition of the Dufour number, an increase in Df translates directly to a decrease in the temperature profiles of the fluid, or to an increase in the concentration profiles of the fluid. An increase in Sc leads to a decrease in the temperature profiles. An increase in Sr causes a decrease in the temperature profiles.

An increase in Eckert number Ec causes an increase in the temperature profiles
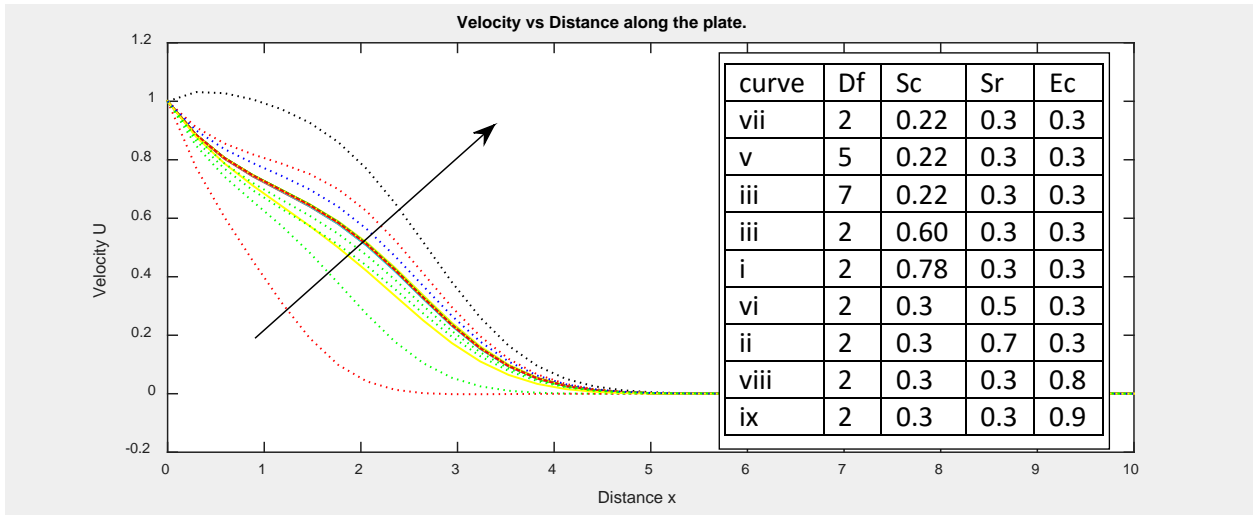
Figure 10: Primaryvelocity profiles for different values of Dufour number Df, Schmidt number Sc, Soret number Sr and Eckert number Ec for $Gr_\theta = -0.5$.
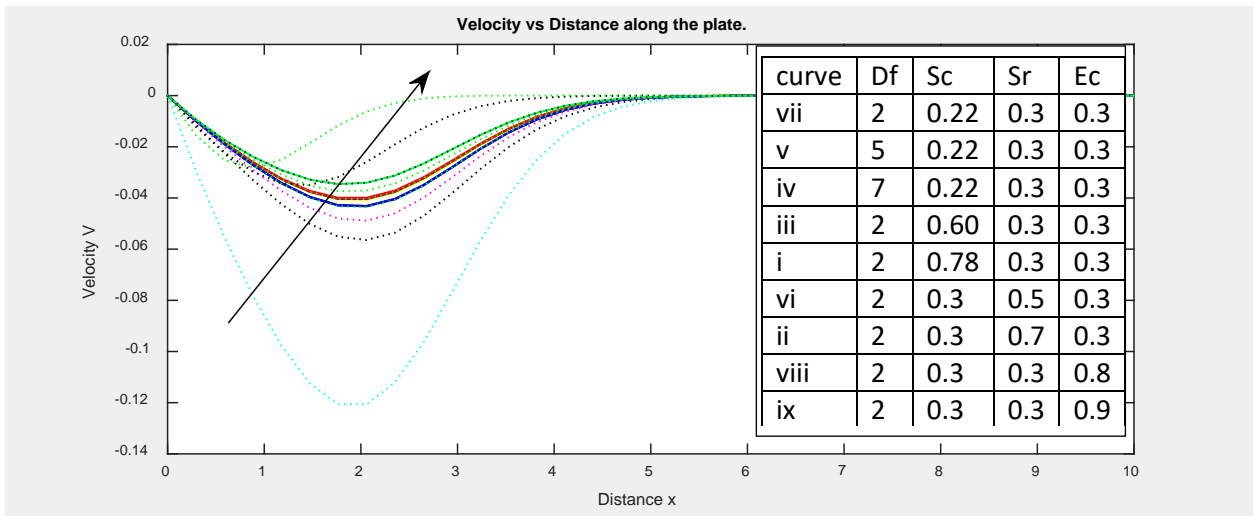
Figure 11: Secondary velocity profiles for different values of Dufour number Df, Schmidt number Sc, Soret number Sr and Eckert number Ec for $Gr_\theta = -0.5$.

From figure 13 it is noted that an increase in Df causes an increase in the concentration profiles. An increase in Schmidt number Sc causes decrease in the concentration profiles. Increase in Schmidt number lead to a decrease of molecular diffusivity, this lead to a decrease of concentration boundary layer. An increase in Sr causes an increase in the concentration profiles. Soret number (Sr) defines the effect of the temperature gradients inducing significant mass diffusion effects. Concentration profiles decrease with increase in the Eckert number.
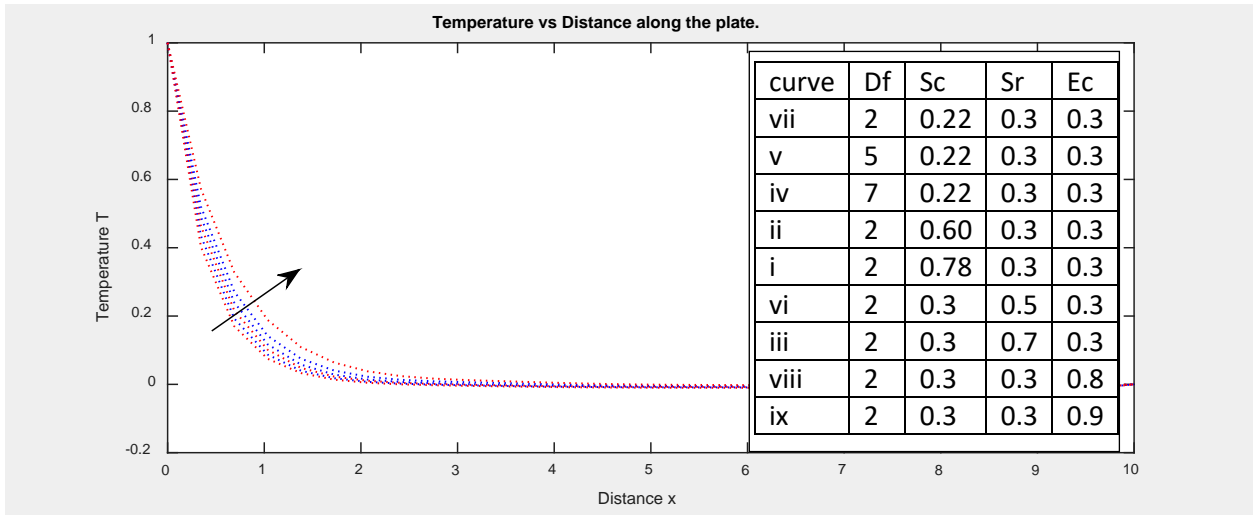
Figure 12: Temperature profiles for different values of Dufour number Df, Schmidt number Sc, Soret number Sr and Eckert number Ec for $Gr_\theta = -0.5$.

curve	Df	Sc	Sr	Ec
vii	2	0.22	0.3	0.3
v	5	0.22	0.3	0.3
iv	7	0.22	0.3	0.3
ii	2	0.60	0.3	0.3
i	2	0.78	0.3	0.3
vi	2	0.3	0.5	0.3
iii	2	0.3	0.7	0.3
viii	2	0.3	0.3	0.8
ix	2	0.3	0.3	0.9
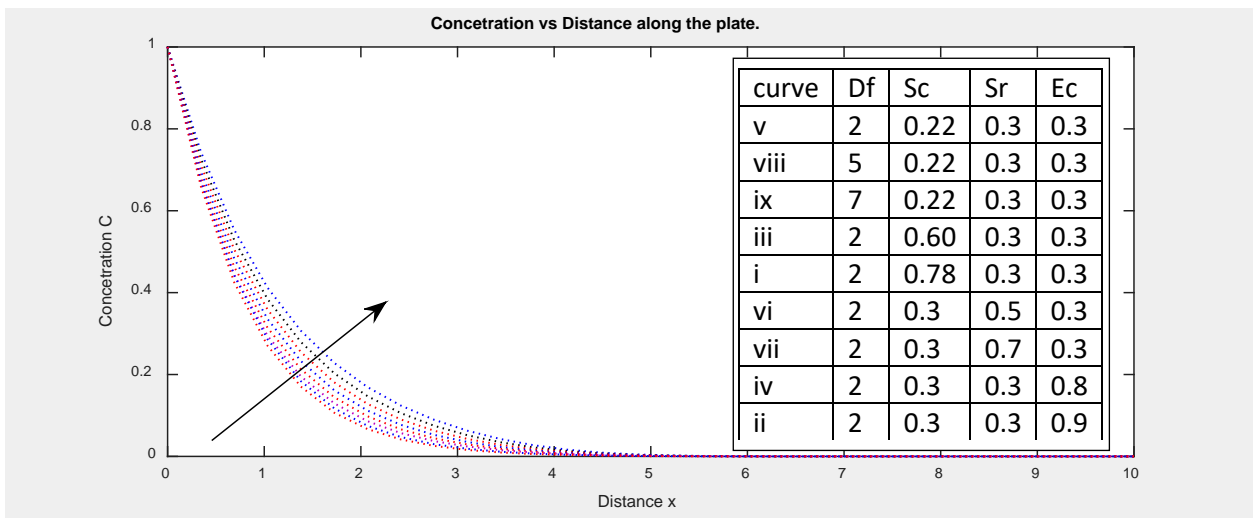
Figure 13: Concentration profiles for different values of Dufour number Df, Schmidt number Sc, Soret number Sr and Eckert number Ec for $Gr_\theta = -0.5$.

curve	Df	Sc	Sr	Ec
v	2	0.22	0.3	0.3
viii	5	0.22	0.3	0.3
ix	7	0.22	0.3	0.3
iii	2	0.60	0.3	0.3
i	2	0.78	0.3	0.3
vi	2	0.3	0.5	0.3
vii	2	0.3	0.7	0.3
iv	2	0.3	0.3	0.8
ii	2	0.3	0.3	0.9

5. Conclusion

An unsteady Magnetohydrodynamic fluid flow past contracting porous surface in a rotating system has been analysed.

The Reynolds number, radiation parameter, time, Eckert number and soret number tend to accelerate fluid flow in both primary, secondary velocity and temperature profiles; reverse effects is observed due to an increase in

rotation, permeability parameter, Dofour, Schmidt number. An increasing in rotation, permeability, radiation parameter, Dofour, soret number increases concentration while reverse effects is observed when Reynolds number, Schmidt number and Eckert number are increased.

The present work can provide basis for further research by considering turbulent flow over a contracting surface.

Acknowledgement

References

[1] Gupta D., Kumar L., Singh B. (2014), "Finite element solution of unsteady mixed convection flow of micropolar fluid over a porous shrinking sheet", The Scientific World Journal, vol. 2014, pp. 11, Article ID 362351,.

[2] Baird R.J., Baird D.T. (1986), "Industrial Plastics", The Goodheart-Willcox Company, Inc., South Holland, Illinois,.

[3] Rafael.C, (2005).Flow and Heat Transfer of a Fluid Through a Porous Medium over a Stretching Surface with Internal Heat Generation/ Absorption and Suction/ Blowing, Fluid Dynamics Research, 37:231–245.

[4] Saritha.S. &P.V. Satya Narayana, (2012). Thermal Diffusion and Chemical Reaction Effects on Unsteady MHD Free Convection Flow Past a Semi Infinite Vertical Permeable Moving Plate, Asian Journal of Current Engineering and Mathematics, 2:131-138

[5] Dawood, A. S and Hmood.B.O., (2006). Steady Free Convection Through Porous Media Enclosing a Rectangular Isothermal Body, Al- Rafidain Engineering,14 (1).

[6] Seethamahalakshim. B.N., Prasad.,G.Raman (2012). MHD Free Convective Mass Transfer Flow Past an Infinite Vertical Porous Plate with Variable Suction and Soret Effect, Asian Journal of Current Engineering and Mathematics, 3:49-55.

[7] Kinyanjui.M., Kwanza. J. k.,Uppal.S.M. (2001). MHD Free Convection Heat and Mass Transfer ofa Heat Generating Fluid Past an Impulsively Started Infinite Vertical Porous Plate with Hall Current and Radiation Absorption, Energy Conversion and Management,42: 917-931.

[8] Shit. G. C., Haldar. R., (2012).Combined Effects of Thermal Radiation and Hall Current on MHD Free-Convective Flow and Mass Transfer over a Stretching Sheet with Variable Viscosity, Journal of Applied Fluid Mechanics, 5:113- 121.

[9] Kangethe. G. Kinyanjui. M &Uppal.S.M. (2012). MHD Flow in Porous Media Over Stretching Surface in A Rotating System with Heat and Mass Transfer, International Electronic Journal of Pure and Applied Mathematics, 4:9-32.

[10] Rakesh K. (2015), studied Combined effects of variable magnetic field and porous medium on the flow of MHD fluid due to exponentially shrinking sheet, International Journal Of Mathematic Archives,6(6):218-226.

[11] Shit. G. C., Haldar. R.,(2011). Effects of Thermal Radiation on MHD Viscous Fluid Flow and Heat Transfer over Non Linear Shrinking Porous Sheet, Applied Mathematics and Mechanics 32 (6):677-688.